Heliyon 10 (2024) e32711

Contents lists available at ScienceDirect

Heliyon

journal homepage: www.cell.com/heliyon

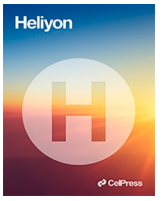

Research article

Investigation of nano MgO loaded polyvinyl chloride polymer in protective clothing as a nonlead materials

Maryam Nasrabadi, Hossein Tavakoli-Anbaran [1,*], Ehsan Ebrahimibasabi [1]

Faculty of Physics and Nuclear Engineering, Shahrood University of Technology, Shahrood, Iran

ARTICLE INFO

Keywords:
Radiation protective clothing
Mass attenuation coefficient
Flux buildup factor
Nanocomposite
Radiation shielding
XCOM
MCNPX

ABSTRACT

Recently, investigation of advanced shielding materials to be used as an alternative to lead apron has become important. In the current study, MgO loaded into PVC matrix as a non-lead modern shielding composite was modeled to evaluate its performance on radiation protective clothing (RPC). Parameters such as mass attenuation coefficient (MAC), mean free path (MFP), flux buildup factor (FBF), transmission factor (TF) and lead equivalent value (LEV) of samples were calculated using MCNPX Code. The simulation of the MCNP code was validated, by comparing the mass attenuation of concrete sample, with standard XCOM data and very good agreement was attended between XCOM and MC Code results. The MAC of nano and micro-sized samples were also compared with pure PVC and it was found that the nano MgO particle exhibits higher attenuation compared to micro MgO particle and pure PVC. The results show that, the MAC of samples increased to 63.13 % in 1.332 MeV with increasing filler concentration of nano MgO to 50 wt% relative to pure PVC. Investigation of LEV shows that nano MgO sample has more effective than Pb in 1.173 and 1.332 MeV gamma ray energy so that it provides 36.46 % and 11.13 % lighter RPC than Pb ones.

1. Introduction

Nowadays, with increasing use of radiation in application areas such as tomography, medicine gamma ray fluorescence studies, nuclear power plant industry, agriculture, space technology, medical imaging, and radiotherapy [1–4], exposing dangerous radiation is possible for worker and patient [5]. So, based on testing novel materials with appropriate properties for radiation protection parameters, radiation such as gamma rays is an essential and important part of protection against radiations in different fields [6–10]. In this regard, Radiation Protective Clothing (RPC) is commonly used against penetration of radiation that used in situations such as diagnostic imaging, accidents during the transportation of radioactive materials and in nuclear facilities [11].

Due to high density, high atomic number, high level of stability and accessibility, lead powder-loaded polymer or elastomer sheets can be considered as the most cost-effective X-ray and gamma shielding material in construction of RPC [12,13]. However, the harmfulness and toxicity of lead material as a shield and protective garment [14], the corrosion and brittleness of lead [15], as well as the objection to the weight of lead clothing [16], led to the investigation of lighter protective materials [17].

Given the type of interactions between materials and gamma rays through a medium, as well as the effectiveness of protection of

* Corresponding author.
E-mail addresses: tavakoli.anbaran@gmail.com, Tavakoli-Anbaran@shahroodut.ac.ir (H. Tavakoli-Anbaran), ehsan.eb.64@gmail.com (E. Ebrahimibasabi).

[1] Both authors contributed equally to the manuscript.

https://doi.org/10.1016/j.heliyon.2024.e32711
Received 27 February 2024; Received in revised form 9 April 2024; Accepted 7 June 2024
Available online 8 June 2024

shielding matter which depend on the energy of gamma rays, attenuation coefficients of the ingredient materials and the thickness of the aprons will be of particular importance for RPC [14,18]. Therefore, early studies were conducted on non-lead materials due to the desire to achieve light weight of RPC and the possibility of improving the protective performance [12].

With development in nano science technology as an advanced scientific branch, radiation protection by nano structure has become useful and practical. Therefore, nano structures have also been studied in the field of ionizing radiation protection [19–21].

Nanoparticles has novel features that can be fabricated in different forms such as polymer nanocomposites by managing the dimensions. In addition, nano-sized structures have high mechanical properties such as elastic stiffness and strength with only a small amount of nano additives [22,23].

Some studies of investigating the influence of particle size in the field of radiation protection performed by authors such as: Dong et al. that evaluated shielding parameter of nano and micro- WO_3 and observed that the influence of nano-sized of WO_3 was more effectual than micro-sized of WO_3 in the epoxy resin [24]. Also, the effective of nano and micro sized of Gd_2O_3 on shielding properties of the pure epoxy resin was investigated by Ran et al., [25]. Alavian et al. studied the effect of (micro and nano) size and proportion of tungsten particles on shielding attributes of light density polyethylene [26]. Nikeghbal et al. investigated the effect of particle size of WO_3 and Bi_2O_3 prototypes on the cone beam computed tomography (CBCT) X-rays radiation protection properties of polymer composite by experimental studies [27].

Also, an investigation of Poly Vinyl Alcohol-lead acetate in a polymer composite as a light and elastic superseded for lead shields performed in 140 keV energy of gamma rays by Aminian et al. and compared the biological effects in nuclear medicine of their composite with conventional lead shields [28]. McCaffrey et al., studied the attenuation of several lead and non-lead materials in x-ray diagnostic imaging energies range of 60–120 kVp, that used in RPC. They resulted various non-Pb materials are sufficient for increasing radiation protection relation to the lead garment. The selection of material depends on the radiation energy for attenuating, and also the most important standard in this field is lead equivalent parameter [14]. Other study is about a soft shield based on a hydrogel that was created by integrating PbO_2 particles into hydrogels with a cross-linking network [17].

Recently, novel composite materials such as metal polymer composites (MPCs) have been used in attenuating gamma rays. The MPCs are composites with a polymer base (matrix) and inorganic filler materials (metal or metal compounds). The improvement of MPCs is attributed to the even distribution of the metal with small-sized particles within a polymer matrix, which provides high strength, flexibility, and cost-effectiveness, along with suitable mechanical properties for the intended use [29–31].

Polyvinyl chloride (PVC), is one of the most widely used thermoplastics due to the low cost of production and processing and resistance to radiation without significant changes in its mechanical properties, so it can be used as an excellent superseded material to make radiation protection materials [32,33]. PVC is a rigid material, that can be a flexible polymer by plasticizing with the way of crosslinking process [34].

Several investigations are performed regarding use of PVC crosslinked by gamma ray as a polymer composite for radiation protection. Investigation of wood-polyvinyl chloride (WPVC) composites with Bi_2O_3 filler for X-ray shielding was performed by Worawat et al. in different contents. Their studies indicated that the X-ray shielding properties of composites enhanced by increasing Bi_2O_3 but decreased at upper contents of wood [35]. Nu~nez-Briones et al., evaluated the shielding properties of PVC composite loaded with tantalum carbide (TaC) against X-Rays at radiodiagnosis energies 50–129 kV [33].

Overall, PVC is incredibly adaptable. By adding different additives, it can be formulated into rigid pipes, flexible sheets, films, and even complex shapes. This versatility allows it to be used in a wide range of applications [36]. Also, PVC is a popular choice for applications requiring high flexibility due to its exceptional elongation strength, surpassing many other thermoplastics. Moreover, PVC is readily available and cost-effective Hence, apart from the aforementioned characteristics, it can be claimed that polymer composites based on PVC, compared to other polymers, can be a suitable material for use in lightweight radiation protective clothing for radiological application.

Among the metal oxide nanoparticle, magnesium oxide (MgO) nanoparticles are widely used in different applications in the chemical industry and are effective on the mechanical, durability and microstructure properties of cement-based materials as an expanding additive [37]. Due to various applications of MgO nanoparticles in the areas of catalysis, refractory materials such as ceramics, electronics and superconductors and contributes excellent flame resistance, it has attracted special attention [38]. Hence, some studies have been made in order to calculate the mass attenuation coefficient of various ores with different weight percentage of MgO by Oto et al. [39]. Also, Hanfi et al. investigated the effect of MgO content on radiation shielding and mechanical properties of tellurite glasses [40].

To the best of the authors' knowledge, there is no investigation on novel shielding materials for using in RPC including MgO added to polymer-based materials. Therefore, in this study, to improve the wearability of RPC, we aim to achieve a lightweight shield. Therefore, we studied the effect of nano/micro MgO on radiation shielding properties of PVC polymer for improving the RPC application. Accordingly, the present study aimed to evaluates the radiation shielding capacity of the polyvinyl chloride polymer loaded with nano and micro metric sizes of MgO using a Monte Carlo code (MC). For this purpose, two different particle sizes including 100 nm and 1 μm were considered. Then, the mass attenuation coefficient (MAC), mean free path (MFP) and flux buildup factor (FBF) of some samples were calculated for radiation shielding of gamma ray sources ^{60}Co (1172 keV, 1332 keV), ^{137}Cs (662 keV), ^{133}Ba (355 keV) and ^{241}Am (59.6 keV). As well as transmission Factor (TF) and 0.5 mm lead equivalent value (LEV) of selected sample for evaluating in RPC application were calculated.

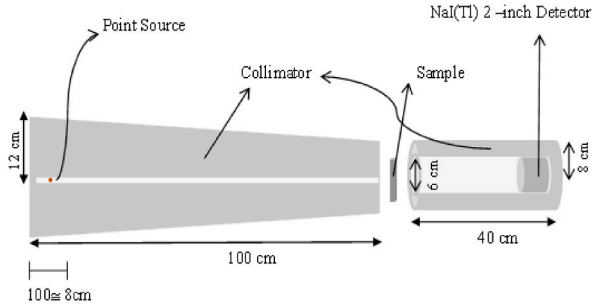

Fig. 1. Design of simulation geometry in MCNPX code.

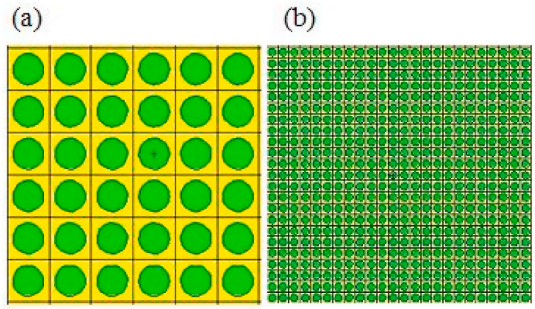

Fig. 2. Schematic design of sample in: a) micro-sized MgO as a sphere with a diameter of 1 μm; b) nano-sized MgO as a sphere with a diameter of 100 nm.

Table 1
Different investigated radii of filler.

Radius of sphere	Unit cell edge (cm)	Number of unit cell in sample (N)
1 μm	2.773×10^{-4} cm	1,688,520,798,491
0.5 μm	1.386×10^{-4} cm	13,508,166,387,930
100 nm	2.773×10^{-5} cm	1,688,520,798,491,264
50 nm	1.386×10^{-5} cm	13,508,166,387,930,114
47 nm	1.034×10^{-5} cm	16,263,456,059,748,459
46 nm	1.012×10^{-5} cm	17,347,341,153,234,818
45 nm	9.904×10^{-6} cm	18,529,720,696,749,127

2. Materials and methods

2.1. MCNPX simulation geometry

In the current study, in order to model the samples and evaluate the important factors like MAC, MFP, FBF, TF and LEV several Monte Carlo calculations were carried out using the MCNPX code. Typically, MCNPX code is used in physical radiations for transport calculations of neutron, photon, and electron [41]. In all simulations, photon and electron transportation mode is used for calculation. We used mono-energetic beams in order to determine the photon mass attenuation coefficients of micro and nano-sized samples. Gamma ray's energy bins lied within range of 0.05 MeV–1.332 MeV. According to Fig. 1, the geometry of interest was simulated, which consists of photon narrow beam as a point source of gamma and lead collimators as well as 2-inch diameter NaI(Tl) detector.

The photon source is located at the end of cone with 100 cm length housed in a cylinder with radius of 0.5 cm and 96 cm height in a conical collimator. Also, the detector is located in a cylinder with 8 cm radius and 40 cm height. Nano and micro structure of materials were located between the source and detector at the distance of 96 cm from the photon source. The attenuator sample was modeled as $2 \times 2 \times 9$ cm^3 cube for the MAC calculations. Also, for better comparisons of attenuation rate, the LEV of all samples consider as thin sheets simulated in g/cm^2, regardless of density of material.

F8 and FT8 tally and Gaussian energy broadening (GEB) card were used to calculate the photon flux within the detector cell which scores the number of photons entering the detector in terms of n/cm^2. As well as, calculating attenuation parameters were performed by evaluated comparing net peak areas in spectra in the presence of sample, and net peak areas in spectra without sample. All the simulations were carried out with a relative error less than 0.3 %.

Table 2
Characteristic of composite matrix in different size and weight percentage of MgO.

MgO size	Weight percentage of MgO (%)	Unit cell edge (cm)	Number of unit cell in sample (N)
1 μm	25	1.747×10^{-4} cm	6,751,865,553,534
	35	1.540×10^{-4} cm	9,856,899,720,283
	50	1.386×10^{-4} cm	13,508,166,387,930
100 nm	25	1.747×10^{-5} cm	6,751,865,553,534,181
	35	1.540×10^{-5} cm	9,856,899,720,283,090
	50	1.386×10^{-5} cm	13,508,166,387,930,114

Table 3
The chemical composition with different weight percentages and density of samples.

Composition of materials		Density (g/cm^3)
Pure PVC	0 wt% MgO[a] 100 wt% PVC[b]	1.406
Lead	–	11.36
Sample1	25 wt% MgO 75 wt% PVC	1.658
Sample2	35 wt% MgO 65 wt% PVC	1.785
Sample3	50 wt% MgO 50 wt% PVC	2.019

[a] Magnesium Oxide.
[b] Polyvinyl Chloride.

2.2. Definition of micro and nano-particles in MCNPX code

The lattice (LAT) and universe (U) cards of MCNP have been used to define micro and nanoparticles. Micro and nano particle fillers of magnesium oxide were simulated as spheres located in the center of the polyvinyl chloride matrix cube (polymer matrix), as displayed in Fig. 2.

For validating MCNP code for simulation of micro and nano particles, different radii of filler sphere is determined as it shown in Table 1. By running the input file, it was shown that filler with radius of 47 nm and higher can be used [42]. So, the diameters of each nano and micro spheres were selected as 100 nm and 1 μm respectively.

The numbers and the edges of each cube of nano and micro sphere which added into the polymer, for the weight percentage of 25, 35 and 50 MgO were calculated according to Table 2. Also, the chemical composition with different weight percentages and density of samples used in the simulations are listed in Table 3. The density of samples (ρ_c) is calculated with bellow equation [26]:

$$\rho_c = \frac{1}{\sum_i^n \left(w_i / \rho_i \right)}$$

where, w_i is the weight fraction of the i-th Constituent in the composite (filler and matrix) and ρ_i is the density of the i-th Constituent in the composite.

2.3. Shielding parameters calculation

Obtaining a suitable radiation protection composite is due to the awareness of proper physical properties of material structure [43]. In gamma rays shielding, effective parameters such as mass attenuation coefficient, flux buildup factor, mean free path, transmission factor and 0.5 mm lead equivalent are investigated.

The mass attenuation coefficient (MAC) as a key parameter in radiation studies, can be determined using the Beer–Lambert law which is formulated as below equations.

$$I = I_0 \, e^{-\mu x} \tag{1}$$

$$\mu_m = \left(\frac{\mu}{\rho} \right) = \frac{\mathrm{Ln}(I_0/I)}{\rho x} \tag{2}$$

where, I and I_0 are the attenuated and incident photon intensity, respectively. x (cm) and ρ (g.cm^{-3}) are the thickness and the density of the attenuator sample (slab). μ (cm^{-1}), μ_m (cm^2.g^{-1}) are linear and mass attenuation coefficients, respectively [44]. This law is valid when the three conditions of monochromatic gamma rays, thin absorbing material and narrow beam geometry are applied [45].

Otherwise, the broad beam geometry may increase the intensity of incident photons due to divergent incident photons from large

Table 4
Differences of MAC (XCOM and MC code and Experimental).

Energy (MeV)	This study (MCNPX)	XCOM	Exp [51].	Difference[a]	Difference[b]
0.663	0.0781 ± 0.003	0.0772	0.0780	0.0117	0.0012
0.778	0.0723 ± 0.004	0.0716	–	0.0097	–
0.964	0.0654 ± 0.006	0.0647	–	0.0107	–
1.112	0.0602 ± 0.007	0.0603	–	0.0013	–
1.170	0.0590 ± 0.001	0.0587	0.0580	0.0051	0.0172
1.332	0.0561 ± 0.003	0.0550	0.0550	0.0196	0.0200

[a] relative difference of MCNPX and XCOM.
[b] relative difference of MCNPX and experimental work.

Table 5
The MAC for Pure PVC (Poly vinyl chloride).

Source	Energy (MeV)	Shield	μ/ρ (cm^2/g)
^{241}Am	0.059	Pure PVC	0.2864
^{133}Ba	0.355	Pure PVC	0.0994
^{137}Cs	0.662	Pure PVC	0.0708
^{60}Co	1.173	Pure PVC	0.0489
	1.332		0.0358

Table 6
The MAC for sample1 (Polymer composition-25 wt% Magnesium Oxide).

Source	Energy (MeV)	Shield	μ/ρ (cm^2/g) Micro	μ/ρ (cm^2/g) Nano	Diff %
^{241}Am	0.059	25 wt% MgO 75 wt% PVC	0.2872	0.2978	3.69
^{133}Ba	0.355	25 wt% MgO 75 wt% PVC	0.1274	0.1303	2.23
^{137}Cs	0.662	25 wt% MgO 75 wt% PVC	0.0709	0.0715	0.84
^{60}Co	1.173	25 wt% MgO 75 wt% PVC	0.0512	0.0569	9.97
	1.332	25 wt% MgO 75 wt% PVC	0.0357	0.0394	9.34

thickness of samples [46]. So, a correction factor called 'Flux Buildup Factor' must be applied to modify the Lambert- Beer law according to equation $I = I_0 Be^{(-\mu_m \rho x)}$ where, B is buildup factor. The total gamma beam hitting the detector consists of two components of the scattered and unscattered beam. The FBF is defined as a ratio of the total transmitted photons reached to the detector (It) to those passed through the sample to the detector without interaction (Iu) and described by equation (3) [47].

$$B = \frac{I_{tot}}{I_u} \tag{3}$$

in order to calculate the flux buildup factor with MCNPX code, gamma rays with energy of E is divided in such a way that length of each interval is equal to 0.001. By calculating the value (I_t) and the value recorded in (E−0.001, E) step for (I_u), total value of tally can be obtained [26].

Also, other parameter is significant for shielding investigation is Mean free path (MFP), that is the average distance between two successive interactions of photon with material. So, the MFP is given by reversing total linear attenuation coefficient that is defined by$1/\mu$ [48].

Furthermore, the investigation of shielding effectiveness based on lead is an important quantity. For this reason, the standard parameter of 0.5 mm "lead equivalent" value (0.5 mmPb LEV) should be calculated. The parameter "lead equivalent" is the thickness for any of the other samples which is required to provide 0.5 mm Pb equivalency [14]. For evaluating this parameter, we should know transmission factor that is an adequate parameter for radiation protection. Transmission Factor is defined as a ratio of flux intensity of photons passing through the sample to the flux intensity obtain to detector without interaction as primary flux [49]. So, in this study, for evaluating standard shielding performance of samples, the TF of the pure Pb and nano sample is calculated for evaluating garment materials and comparison with the common standards of 0.5 mm "lead equivalent".

Table 7
The MAC for sample2 (Polymer composition-35 wt% Magnesium Oxide).

Source	Energy (MeV)	Shield	μ/ρ (cm^2/g) Micro	μ/ρ (cm^2/g) Nano	Diff %
^{241}Am	0.059	35 wt% MgO 65 wt% PVC	0.2843	0.3260	12.79
^{133}Ba	0.355	35 wt% MgO 65 wt% PVC	0.1369	0.1466	10.40
^{137}Cs	0.662	35 wt% MgO 65 wt% PVC	0.0713	0.0771	7.52
^{60}Co	1.173	35 wt% MgO 65 wt% PVC	0.0561	0.0632	11.23
	1.332	35 wt% MgO 65 wt% PVC	0.0387	0.0430	10.00

Table 8
The MAC for sample3 (Polymer composition-50 wt% Magnesium Oxide).

Source	Energy (MeV)	Shield	μ/ρ (cm^2/g) Micro	μ/ρ (cm^2/g) Nano	Diff %
^{241}Am	0.059	50 wt% MgO 50 wt% PVC	0.2867	0.3747	23.48
^{133}Ba	0.355	50 wt% MgO 50 wt% PVC	0.1402	0.1467	4.43
^{137}Cs	0.662	50 wt% MgO 50 wt% PVC	0.0844	0.0885	4.63
^{60}Co	1.173	50 wt% MgO 50 wt% PVC	0.0681	0.0718	5.15
	1.332	50 wt% MgO 50 wt% PVC	0.0522	0.0584	10.62

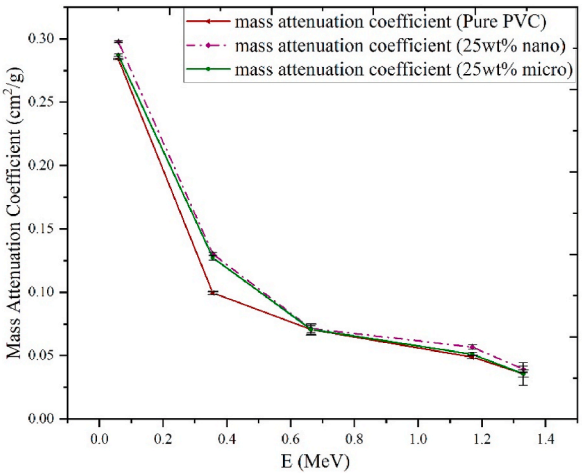

Fig. 3. Comparison of the MAC for micro- and nano-sized particles of sample 1 (Polymer composite with 25 wt% MgO).

3. Results and discussion

3.1. Validation of MCNPX codes

The Monte Carlo (MC) code simulation results were validated by comparing with standard XCOM data and experimental measurements of work ref of [50]. For this purpose, the MAC of concrete sample were calculated in the photon energy range of 0.663–1.332 MeV as shown in Table 4. It can be seen that the maximum difference between the Monte Carlo results, XCOM data and experimental work [51] is 0.01961 and 0.02, respectively. The experimental data of ref [51] has an error of less than or equal to 2 %.

3.2. Efficiency of photon shielding

Calculations of the MAC of samples at photon energies of 0.059, 0.355, 0.662, 1.173, and 1.332 MeV are reported in Tables 5–8. The samples included micro and nano-sized particles with different weight percentages of 25, 35, and 50 wt% of magnesium oxide and

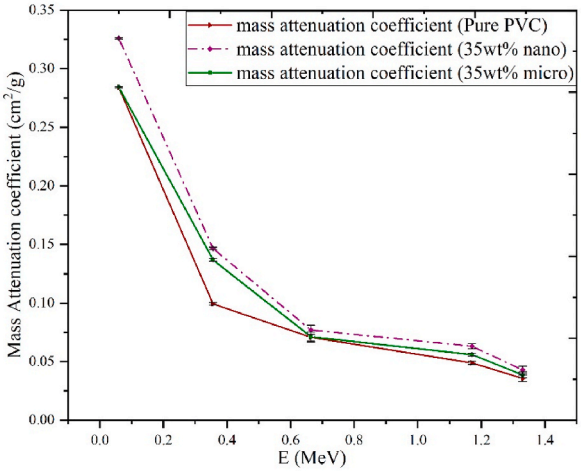

Fig. 4. Comparison of the MAC for micro- and nano-sized particles of sample 2 (Polymer composite with 35 wt% MgO).

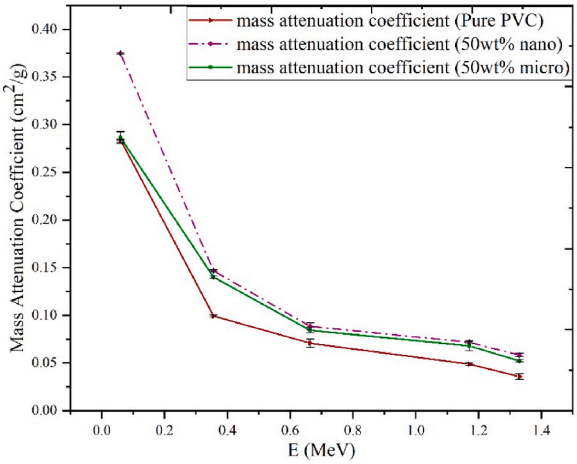

Fig. 5. Comparison of the MAC for micro- and nano-sized particles of sample 3 (Polymer composite with 50 wt% MgO).

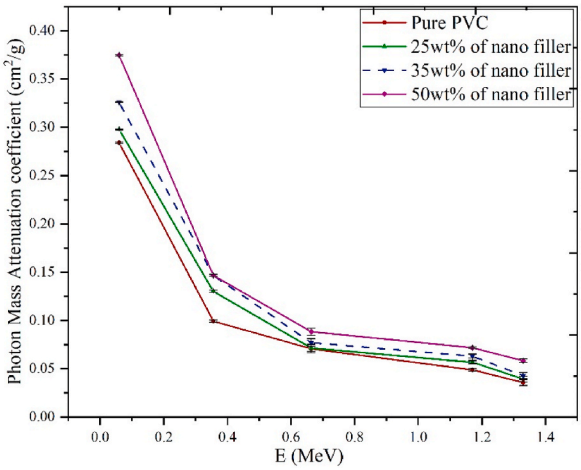

Fig. 6. The variation of the MAC of MPCs with energy (MeV) for nano-sized particles of four samples (Polymer composite with 25, 35 and 50 wt % MgO).

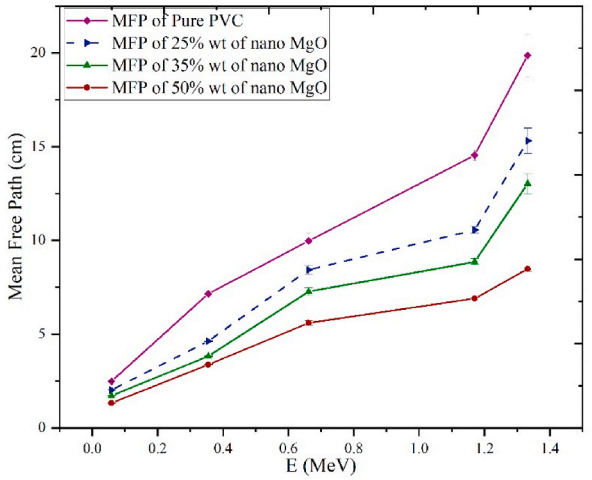

Fig. 7. Comparison of the MFP for nano-sized particles of four samples (pure PVC and Polymer composite with 25, 35 and 50 wt% MgO).

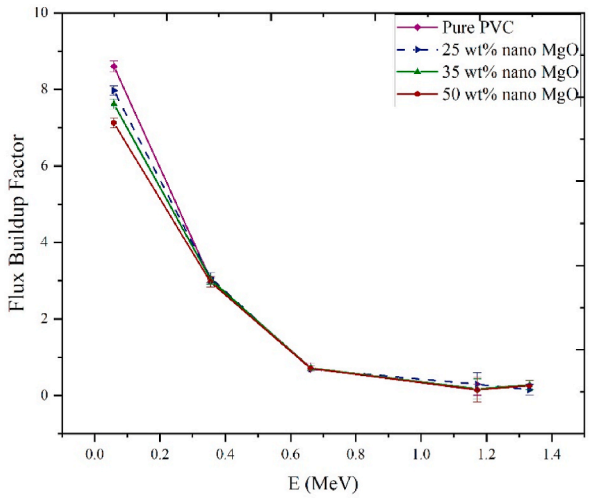

Fig. 8. Variation of flux Buildup Factor with energy (MeV) for 25, 35 and 50 wt% of nano MgO and pure PVC (Polymer composite with 25, 35 and 50 wt% MgO).

pure PVC.

According to the results, the MAC of nano-sized particles of MgO loaded into PVC matrix is higher than that of the micro-sized and pure PVC ones. According to calculations; the MAC of the pure PVC were increased from 0.20 % to 31.09 %, 8.13 % to 44.48 % and 24.12 % to 63.13 % for increment of 25 wt%, 35 wt% and 50 wt% nano MgO within the energy range of 0.059 MeV–1.332 MeV, respectively.

Also, the influence of changing from micro to nano-sized MgO in the enhancement of the MAC from 0.84 % to 9.97 %, for weight percentage of 25 wt% of MgO sample, obtained. For sample2 (35 wt %) and sample3 (50 wt %), the attenuation increase rates were from 7.52 % to 12.79 % and 4.43 % to 23.48 %, which are shown in Tables 6–8, respectively. From the obtained results it can be concluded, the nano-MgO is more effective than micro-MgO in the PVC-based radiation shielding materials. In addition, we found that the MAC of photons on the nano scale of MgO-Polymer composite was increased with increasing in filler proportion from 25 wt% to 50 wt%.

Figs. 3–5 depicts the change of the MAC values versus the incident gamma photon energy for nano and micro-sized MgO. According to the figures, the MAC of the samples decreases with the increase of the energy due to the photoelectric effect, Compton Effect, and pair production. As it shown in the figures, Nanocomposites outperform microcomposites and pure PVC in terms of radiation shielding in the energy range of 0.05–1.332 MeV, due to two factors: the uniform distribution and high specific surface area of the nano-MgO loaded to PVC.

Fig. 6 displays the comparison of the MAC for pure PVC and concentrations of 25 wt%, 35 wt%, and 50 wt% of nano filler in the composite versus various gamma photon energies. It's clear that with increasing of nano filler proportion to 50 wt%, the MAC values

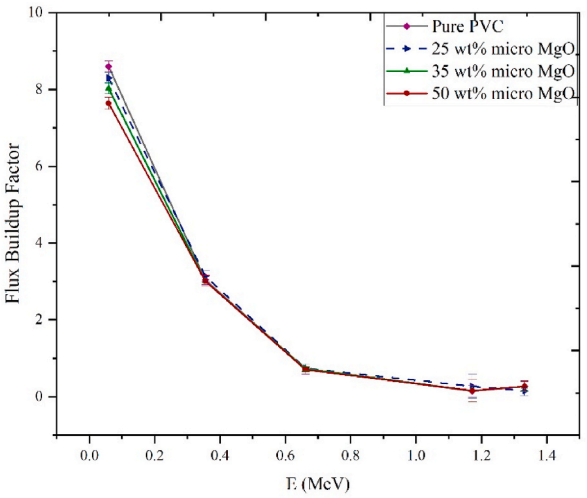

Fig. 9. Variation of flux Buildup Factor with energy (MeV) for 25, 35 and 50 wt% of micro MgO and pure PVC (Polymer composite with 25, 35 and 50 wt% MgO).

increased in term of photons energy, due to photon interactions with nano element of Magnesium as nano filler in PVC matrices. Also, it is observed that the relative difference of the MAC of pure PVC sample to 50 wt% MgO-PVC composite at an energy range of 0.059 MeV–1.332 MeV was equal to 23.6 %, 32.2 %, 19.4 %, 31.9 % and 38.7 %, respectively. Also, the relative difference of 25 wt% MgO-PVC composite to 50 wt% MgO-PVC composite was equal to 20.6 %, 11.2 %, 19.2 %, 20.5 %, and 32.5 %, respectively. These relative differences for 35 wt% MgO-PVC composite to 50 wt% MgO-PVC composite was equal to 13.0 %, 0.07 %, 12.9 %, 12.0 %, and 26.4 %, respectively. Moreover, for all proportion of nano filler and pure PVC during increasing energy from 0.05 to 1.332 MeV, the MAC value is decreasing because of high probability of scattering photons in high energy relative to low energy of photon.

The Mean free path (MFP) attained versus photon energy for four samples is shown in Fig. 7. It is clear that the increase in the amount of weight percentage of nano MgO leads to higher probability of photon interaction and as a result less distance travelled by the photon between two continuous events. As we know, Materials with lower MFP offer more beneficial radiation protection of materials. So, it's obvious from Fig. 7, sample with 50 wt% weight percentage of nano MgO is better than other proportion of nano MgO and Pure PVC.

Furthermore, another important shielding parameter as buildup factor, investigated via MCNPX code [52] for all weight percentage of filler. The flux buildup factor versus various gamma photon energies for pure PVC and polymer composite of nano and micro MgO was calculated. The variation of the FBF respect to the energy has been shown in Figs. 8–9. It is clear that the FBF is strongly decreased in the range of 0.059–1.332 MeV for both micro and nano MgO composite. According to Figs. 8 and 9, the FBF value of the nano composite is lesser than micro ones and pure PVC. Also, as it obvious from figure, the higher proportion on filler for both nano and micro is effective and higher weight percentage of Mg element cause the increase of radiation protection. Hence, from figures, it can understand that nano MgO filler in PVC has more significant shielding properties than micro and pure PVC.

Obviously, at low energies the filler concentration is more effective on the FBF of micro and nano MgO samples and it's nearly constant in high energy region from 0.662 to 1.332 MeV. As it shown in Figs. 8 and 9, FBF has maximum value in energy of 0.05 MeV and decreased with increasing energy. In energy region of 0.05–0.662 MeV, the probability of photon to escape from sample is resulted due to Compton scattering and so the value of FBF is slowly decreased for both micro and nano composites. And then, from 0.662 up to 1.332 MeV, the FBF has low values that it is due to dominance of pair production for absorption of photon.

The results show that, the maximum value of FBF with increment of micro and nano MgO to pure PVC change from 8.60 to 7.97, 7.65 and 7.12 for increasing weight percentage of 25 wt%, 35 wt% and 50 wt% of nano MgO and change from 8.60 to 8.30, 8.03 and 7.64 for increasing weight percentage of 25 wt%, 35 wt% and 50 wt% of micro MgO, respectively.

3.3. Lead equivalent parameter calculation

Finally, the parameter of transmission factor which is the division of intensity photon passing via sample and the photon intensity without interaction calculated for evaluating 0.5mmPb lead equivalent value. So, after selecting of the proper nano sample respect to micro and pure PVC, calculating TF with weight percentage of 25–50 wt% were done in the energy range of 0.059–1.332 MeV for various thickness of 0.1–1 cm. As it shown in Fig. 10(a–e) the TF decrease with increasing weight percentage of nano MgO from 25 wt to 50 wt%. also, TF value of all samples decrease linearly by increasing of thickness and among all samples, nanocomposite with 50 wt % of nano MgO has lower TF value. So, the nano MgO with 50 wt% was selected for calculating of the LEV in different gamma energy range. Also, for better evaluation for evaluating garment materials these values compared with TF value of the 0.5 mm pure Pb.

After investigation of the TF (Transmission Factor) values of the samples, a two-step approach is proposed. The first step involves determining the 0.5 mm lead equivalent value for the Pb sample. This value can be calculated by multiplying the density of Pb (11.36

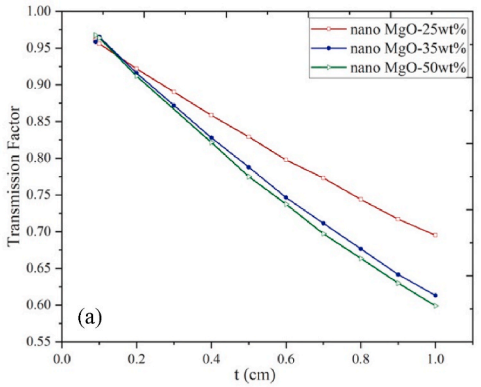

Transmission factor vs thickness for nano-sized particles of samples at the 0.059 MeV gamma ray.

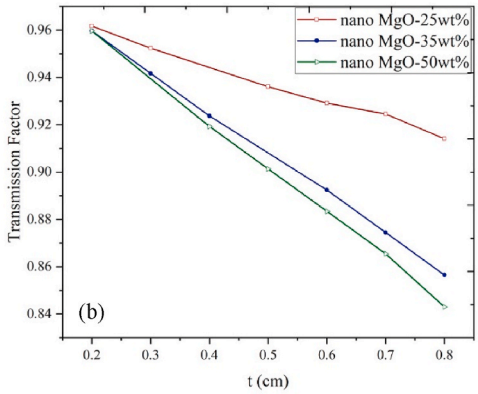

Transmission factor vs thickness for nano-sized particles of samples at the 0.3359 MeV gamma ray.

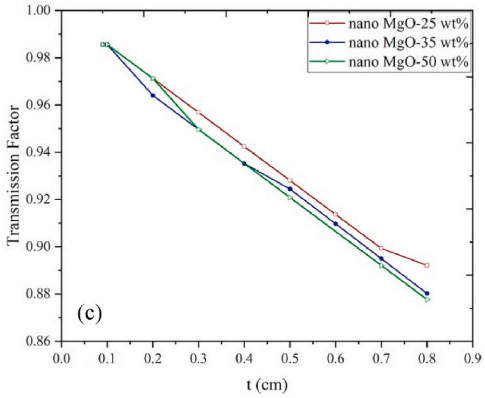

Transmission factor vs thickness for nano-sized particles of samples at the 0.662 MeV gamma ray.

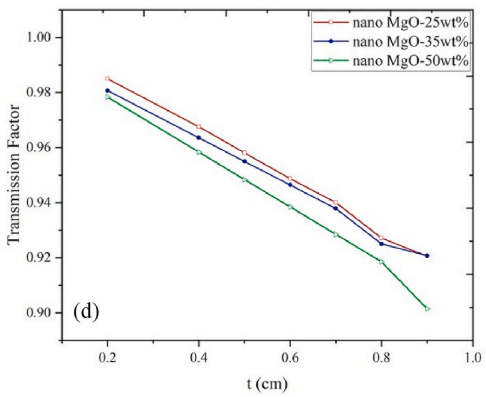

Transmission factor vs thickness for nano-sized particles of samples at the 1.173 MeV gamma ray.

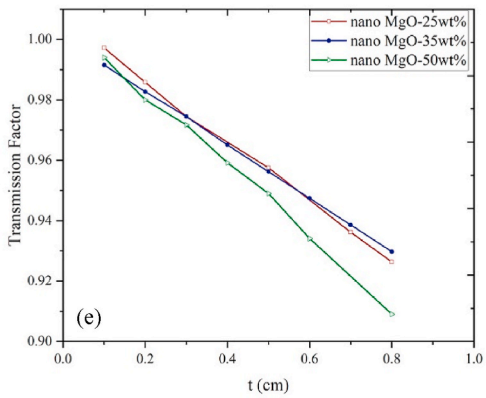

Transmis sion factor vs thickness for nano-sized particles of samples at the 1.332 MeV gamma ray.

Fig. 10. Variation of Transmission factor with thickness for 25, 35 and 50 wt% of nano MgO at the energy range of 0.059–1.332 MeV.

g/cm^3) by the thickness of 0.5 mm, resulting in a value of 0.568 g/cm^2. By expressing the thickness in terms of grams per square centimeter (g/cm^2), a direct assessment of the attenuation abilities of the samples can be made, eliminating the influence of their individual densities. Subsequently, the TF value of the 0.5 mm Pb thickness will be calculated as a reference point for evaluating the equivalent thickness of nano MgO samples in terms of 0.5 mm Pb equivalence. This conversion forms the basis for assessing the attenuation characteristics of the nano MgO sample, independent of each material's unique density.

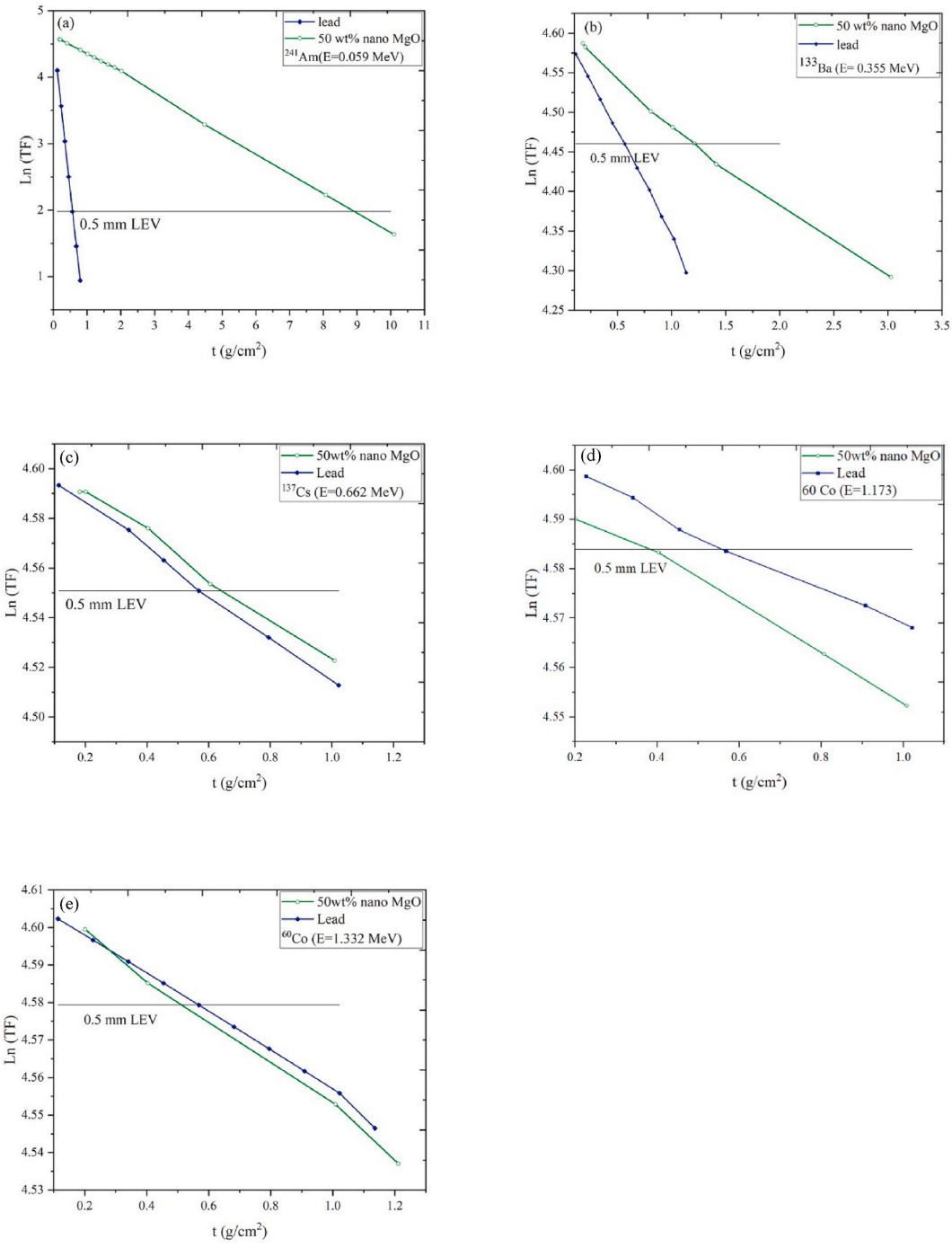

Fig. 11. Variation of Ln (TF) values with thickness in (g/cm^2) for the: a) ^{241}Am, b) ^{133}Ba, c) ^{137}Cs, (d and e) ^{60}Co gamma sources for calculating 0.5 mm LEV of a selected sample.

For this thickness, the Ln (TF) value of Pb in 241-Am source energy is 1.98 that as it seen in Fig. 11, it is shown with horizontal line across the graph. Where the line passes the graph of nano sample, it is equal to 0.5 mm LEV that should be used in RPCs.

As it shown in Fig. 11(a) −11(e), calculated 0.5 mm LEV for energy range of 241-Am, 133-Ba, 137-Cs and 60-Co is equal to 4.46 cm, 6.40 mm, 3.40 mm, 1.90 mm and 2.50 mm, respectively. It is found from result that the nano MgO with 0.5 wt is not as effective for low energy from 0.059 to 0.662 MeV because of the lower dominant of photoelectric effect $\left(\sigma_{ph} \sim const\ \frac{Z^n}{E_\gamma^m}\right)$ of the sample than pure Pb. However, at the energy of 60-Co (1.173–1.332 MeV) is more effective than Pure Pb due to dominance of Compton scattering cross

section in intermediate and high energy region and photon energy is mainly reduced through interaction with electrons via Compton scattering. also, Compton scattering is almost independent of the atomic number of the substance and it can be a good choice as a non-lead RPCs in high energy range of gamma rays. So, a nano MgO sample with 50 wt% can provide a RPC with 36.46 % and 11.13 % lower weight than Pb garments in energy rang of 1.173 and 1.332 MeV, respectively.

4. Conclusions

In the present study, the impact of particle sizes and percentages of magnesium oxide on the gamma radiation shielding properties MAC, FBF, MFP, TF and 0.5 mm Pb LEV of Polyvinyl Chloride in radiation protective clothing has been investigated. Different weight percentage of 25 wt%, 35 wt%, and 50 wt% of nano and micro MgO loaded into polyvinyl chloride base (polymer-based material) using MCNPX code. Nano-sized MgO with 50 wt% proportion showed better photon attenuation compared to micro-sized and pure PVC samples due to uniform distribution of MgO nanoparticles. The MAC was enhanced in the energy range of 0.059–1.332 MeV with increasing filler proportion.

Moreover, the main conclusions can be summarized as follows:

1 The photon shielding capability of sample.3 relatives to pure PVC has increased of 30.81 %, 32.24 %, 24.12 %, 46.83 % and 38.70 % for energy of 0.059, 0.355, 0.662, 1.173 and 1.332 MeV, respectively. The enhancement of the MAC from micro to nano-sized MgO were calculated and the attenuation increase rates were from 0.84 % to 9.97 %, for weight percentage of 25 wt% of MgO sample, 7.52 % to 12.79 % and 4.43 % to 23.48 % for weight percentage of 35 wt% and 50 wt%, respectively.
2 The results of flux buildup factor showed that, increasing the filler concentration is more effective in the low energy region than the high energy region. Also, Transmission factor decreased with increasing nano MgO weight percentage, and the 50 wt% of nano MgO was used for calculating 0.5 mm lead equivalent value due to its low TF value.
3 0.5 mm lead equivalent value of nano 50 wt MgO sample was calculated with transmission factor values in all energy ranges. The results show that the studied sample has higher efficiency in the term of shielding effect than pure pb in high energy of gamma rays. As it provides a RPC with 36.46 % and 11.13 % lighter than Pb garments in energy rang of 1.173 and 1.332 MeV, respectively.

Overall, it would be useful to apply PVC/nano composite as a novel shielding material, because it can provide a light-weight RPC at high energy region of photons. Also, we are in the process of making a laboratory prototype and measuring the experimental results and can measure the mechanical properties as tensile test, measuring young modulus etc. of selected sample for using in future studies.

Data availability statement

The data that support the findings of this study are available from the corresponding author (tavakoli.anbaran@gmail.com, Tavakoli-Anbaran@shahroodut.ac.ir), upon reasonable request.

CRediT authorship contribution statement

Maryam Nasrabadi Writing – review & editing. **Hossein Tavakoli-Anbaran** Writing – review & editing. **Ehsan Ebrahimibasabi:** Writing – review & editing.

Declaration of competing interest

The authors declare that they have no known competing financial interests or personal relationships that could have appeared to influence the work reported in this paper.

References

[1] F. Zhang, H. Wu, X. Wang, G. Wu, W. Jia, Y. Ti, "Compact shielding design of a portable 241Am–Be source, Appl. Radiat. Isot. (2017) 49–54, https://doi.org/10.1016/j.apradiso.2017.06.033.
[2] M.M. Rafiei, H. Tavakoli-Anbaran, Study of exposure buildup factors with detailed physics for cobalt-60 gamma source in water, iron, and lead using the MCNPX code, Eur. Phys. J. Plus 133 (2018) 548, https://doi.org/10.1140/epjp/i2018-12355-8.
[3] S.O. Shamsan, M.I. Sayyed, D.K. Gaikwad, P.P. Pawar, Attenuation coefficients and exposure buildup factor of some rocks for gamma ray shielding applications, Rad. Phys. Chem. 148 (2018) 86–94, https://doi.org/10.1016/j.radphyschem.2018.02.026.
[4] I.S. Mahmoud, A.M. Issa Shams, Y.B. Saddeek, H.O. Tekin, O. Kilicoglu, T. Alharbi, M.I. Sayyed, T.T. Erguzel, R. Elsaman, Gamma, neutron shielding and mechanical parameters for lead vanadate glasses, Ceram. Int. 45 (2019) 14058–14072, https://doi.org/10.1016//j.ceramint.2019.04.105.
[5] C.K. Seon, R.C. Jeong, K.J. Byeong, Physical analysis of the shielding capacity for a lightweight apron designed for shielding low intensity scattering X-rays, Sci. Rep. (2016) 27721, https://doi.org/10.1038/srep27721.
[6] K. Celal, G. Meng, G. Seda, G. Yasin, A.P. Khursheed, O.Y. Ali, Measurement on the neutron and gamma radiation shielding performance of boron-doped titanium alloy Ti50Cu30Zr15B5 via arc melting technique, Heliyon 9 (2023) e21696, https://doi.org/10.1016/j.heliyon.2023.e21696, 1-11.
[7] M. Nasrabadi, E. EbrahimiBasabi, H. Tavakoli-Anbaran, Compact shielding and irradiator design of a ^{252}Cf neutron source, Appl. Radiat. Isot. 143 (2019) 29–34, https://doi.org/10.1016/j.apradiso.2018.10.005.
[8] K.A. Mahmoud, M.I. Sayyed, O.L. Tashlykov, Gamma ray shielding characteristics and exposure buildup factor for some natural rocks using MCNP-5 code, Nucl. Eng. Technol. 51 (2019) 1835–1841, https://doi.org/10.1016/j.net.2019.05.013.

[9] D.K. Gaikwad, M.I. Sayyed, S.N. Botewad, S. Obaid Shamsan, Z.Y. Khattari, U.P. Gawai, F. Afaneh, M.D. Shirshat, P.P. Pawar, Physical, structural, optical investigation and shielding featuresof tungsten bismuth tellurite-based glasses, J. Non-Cryst. Solids (2019) 158–168, https://doi.org/10.1016/j.jnoncrysol.2018.09.038.

[10] D.I. Tishkevich, T.I. Zubar, A.L. Zhaludkevich, I.U. Razanau, T.N. Vershinina, A.A. Bondaruk, E.K. Zheleznova, M. Dong, M.Y. Hanfi, M.I. Sayyed, M.V. Silibin, S. V. Trukhanov, A.V. Trukhanov, Isostatic hot pressed W–Cu composites with nanosized grain boundaries: microstructure, structure and radiation shielding efficiency against gamma rays, Nanomaterials 1–14 (12) (2022) 1642, https://doi.org/10.3390/nano12101642.

[11] K. Michaela, S. Jaroslav, O. Petr, Measuring and Monte Carlo modelling of X-ray and gamma-ray attenuation in personal radiation shielding protective clothing, Comput. Math. Methods Med. (2019) 1–9, https://doi.org/10.1155/2019/1641895.

[12] E.W. Webster, Experiments with medium Z materials for shielding against low-energy x-rays, Radiology 86 (1966) 146.

[13] M.M. Movahedi, A. Abdi, A. Mehdizadeh, N. Dehghan, E. Heidari, Y. Masumi, M. Abbaszadeh, Novel paint design based on nanopowder to protection against X and gamma rays, Indian J. Nucl. Med. 23 (2014) 18–21, https://doi.org/10.4103/0972-3919.125763.

[14] J.P. McCaffrey, H. Shen, B. Downton, E. Mainegra-Hing, Radiation attenuation by lead and nonlead materials used in radiation shielding garments, Med. Phys. 34 (2008) 530–537, https://doi.org/10.1118/1.2426404.

[15] D.K. Schick, R.N. Casey, L.H. Sim, K.J. Siddle, Corrosion of lead shielding in a radiology department, Australas. Radiol. 43 (1) (1999) 47–51, https://doi.org/10.1046/j.1440-1673.1999.00611.x.

[16] M.J. Yaffe, et al., Composite materials for x-ray protection, Health Phys. 60 (1991) 661–664, https://doi.org/10.1097/00004032-199105000-00004.

[17] S.H. Gwon, J.H. Oh, M. Kim, S. Choi, K.H. Oh, J.Y. Sun, Sewable soft shields for the γ-ray Radiation, Sci. Rep. 8 (2018) 1852, https://doi.org/10.1038/s41598-018-20411-3.

[18] R.D. Evans, The Atomic Nucleus, Mcgraw-Hill, New York, 1955.

[19] H.O. Tekin, V.P. Singh, T. Manici, Effects of micro-sized and nano-sized WO_3 on mass attenuation coefficients of concrete by using MCNPX code, Appl. Radiat. Isot. (2017) 21–22, https://doi.org/10.1016/j.apradiso.2016.12.040.

[20] A. Mesbahi, H. Ghiasi, Shielding properties of the ordinary concrete loaded with micro- and nano-particles against neutron and gamma radiations, Appl. Radiat. Isot. 136 (2018) 27–31, https://doi.org/10.1016/j.apradiso.2018.02.004.

[21] Y. Karabul, O. Içelli, The assessment of usage of epoxy based micro and nano structured composites enriched with Bi_2O_3 and WO_3 particles for radiation shielding, Results Phys. 26 (2021) 104423, https://doi.org/10.1016/j.rinp.2021.104423.

[22] M. Singh, S. Manikandan, A.K. Kumaraguru, Nanoparticles: a new technology with wide applications, Res. J. Nano sci. and Nanotech 1 (2011) 1–11, https://doi.org/10.3923/rjnn.2011.1.11.

[23] A.G. Nunez-Briones, R. Benavides, E. Mendoza-Mendoza, M.E. Martinez-Pardo, H. Carrasco-Abrego, C. Kotzian, F.R. Saucedo-Zendejo, L.A. Garcia-Cerda, Preparation of PVC/Bi_2O_3 composites and their evaluation as low energy X-Ray radiation shielding, Radiat. Phys. Chem. 179 (2021) 109198, https://doi.org/10.1016/j.radphyschem.2020.109198.

[24] Y. Dong, S.Q. Chang, H.X. Zhang, C. Ren, B. Kang, M.Z. Dai, Y.D. Dai, Effects of WO3 particle size in WO3/Epoxy resin radiation shielding material, Chin. Phys. Lett. 29 (2012), https://doi.org/10.1088/0256-307X/29/10/108102.

[25] L. Ran, Gu Yizhuo, W. Yidong, Yang Zhongjia, Li Min, Z. Zuoguang, Effect of particle size on gamma radiation shielding property of gadolinium oxide dispersed epoxy resin matrix composite, Mater. Res. Express 4 (2017) 1–11, https://doi.org/10.1088/2053-1591/aa6651.

[26] H. Alavian, H. Tavakoli-Anbaran, Study on gamma shielding polymer composites reinforced with different sizes and proportions of tungsten particles using MCNP code, Prog. Nucl. Energy 115 (2019) 91–98, https://doi.org/10.1016/j.pnucence.2019.03.033.

[27] K. Nikeghbal, Z. Zamanian, S. Shahidi, G. Spagnuolo, P. Soltani, "Designing and fabricating nano-structured and micro-structured radiation shields for protection against CBCT exposure, Materials 13 (2020) 1–11, https://doi.org/10.3390/ma13194371.

[28] M. Aminian, M. Bakhshandeh, M. Allahbakhshian-Farsani, E. Bakhshandeh, N. Shakeri, Comparison of the protection performance in a composite shield and a lead standard shield in terms of biological effects in nuclear medicine, Iran. J. Nucl. Med. (2017) 12–135.

[29] W.S. Khan, N.N. Hamadneh, W.A. Khan, Polymer nanocomposites – synthesis techniques, classification and properties, book: science and applications of tailored nanostructures, One Central Press (OCP) (2016) 50–67 (Chapter 4).

[30] J. Kim, D. Seo, B.C. Lee, Y.S. Seo, W.H. Miller, Nano-W dispersed gamma radiation shielding materials, Adv. Eng. Mater. 16 (2014) 1083–1089, https://doi.org/10.1002/adem.20140027.

[31] N. Shruti, K. O.sei Ernest, T.W.Y. John, Polymer nanocomposite-based shielding against diagnostic X-rays, J. Appl. Polym. Sci. (2012) 8, https://doi.org/10.1002/app.37980.

[32] J.G. Drobny, Ionizing Radiation and Polymers: Principles, Technology and Applications, William Andrew, Norwich, 2012.

[33] A.G. Nu~nez-Briones, R. Benavides, M.E. Martínez-Pardo, H. Carrasco-Abrego, C. Kotzian-Pereira-Benavides, D. Espejo-Villalobos, L.A. García-Cerda, Effect of gamma dose rate in the crosslinking of PVC composites used for radiation protection in radiology, Radia. Phys. Chem. 191 (2022) 109866, 10.106/j.radphysschem.2021.109866.

[34] P.H. Sang, J.P. Kyung, W.L. Kyung, Crosslinked PVC polymerization: study on process dependencies, J. Appl. Polym. Sci. 83 (2002) 1947–1954, https://doi.org/10.1002/app.10109.

[35] W. Poltabtim, E. Wimolmala, T. Markpin, N. Sombatsompop, V. Rosarpitak, K. Saenboonruang, X-Ray shielding, mechanical, physical, and water absorption properties of wood/PVC composites containing bismuth oxide, Polymers 13 (13) (2021) 2212, https://doi.org/10.3390/polym13132212.

[36] N. Ranjan, Chitosan with PVC polymer for biomedical applications: a bibliometric analysis, Mater. Today: Proc. 894–898 (2021), https://doi.org/10.1016/j.matpr.2021.04.274.

[37] R. Polat, R. Demirbog, F. Karagöl, The effect of nano-MgO on the setting time, autogenous shrinkage, microstructure and mechanical properties of high performance cement paste and mortar, Construct. Build. Mater. 156 (2017) 208–218, https://doi.org/10.3390/ma14133766.

[38] M.R. Bindhu, M. Umadevi, M.K. Micheal, M.V. Arasu, N.A. Al- Dhabi, Structural, morphological and optical properties of MgO nanoparticles for antibacterial applications, Mater. Lett. 166 (2016), https://doi.org/10.1016/j.matlet.2015.12.020.

[39] B. Oto, N. Yıldız, F. Akdemir, E. Kavaz, Investigation of gamma radiation shielding properties of various ores, Prog. Nucl. Energy 85 (2015) 391–403, https://doi.org/10.1016/j.pnucene.2015.07.016.

[40] M.Y. Hanfi, M.I. Sayyed, Eloic Lacomme, K.A. Mahmoud, I. Akkurt, The influence of MgO on the radiation protection and mechanical properties of tellurite glasses, NET 53 (2021) 2000–2010, https://doi.org/10.1016/j.net.2020.12.012.

[41] D.B. Pelowitz, MCNPX User's Manual Version 2.6.0, LA-CP-07-1473, 2008.

[42] D.B. Pelowitz, MCNPX User's Manual Version 2.6.0, LA-CP-07-1473, 5–1vols. 8–19, 2008.

[43] S.O. Shamsan, M.I. Sayyed, D.K. Gaikwad, H.O. Tekin, Y. Elmahroug, P.P. Pawar, Photon attenuation coefficients of different rock samples using MCNPX, Geant4 simulation codes and experimental results: a comparison study, Radiat. Eff. Defect Solid 173 (2018) 900–914, https://doi.org/10.1080/10420150.2018.1505890.

[44] D. Yılmaza, M. Buyukyıldız, Calcium-based TLD materials for radiation applications, radiat. phys. chemi. 179 (2020) 109196, https://doi.org/10.1016/j.radphyschem.2020.109196.

[45] P.V. Singh, N.M.m. Badiger, A comprehensive study on gamma-ray exposure build-up factors and fast neutron removal cross sections of fly-ash bricks, hindawi publishing corporation, Journal of Ceramics (2013) 967264, https://doi.org/10.1155/2013/967264.

[46] A.E. Ersundu, M. Büyükyıldız, M.Ç. Ersundu, E. Şakar, M. Kurudirek, The heavy metal oxide glasses within the WO_3-MoO_3-TeO_2 system to investigate the shielding properties of radiation applications, Prog. Nucl. Energy (2018) 1–8, https://doi.org/10.1016/j.pnucene.2017.10.008.

[47] N.T. Soulfanidis, Measurement and Detection of Radiation, fourth ed., University of Missouri-Rolla, 2015.

[48] A.M. El-Khayatt, A.M. Ali, V.P. Singh, Photon attenuation coefficients of Heavy-Metal Oxide glasses by MCNP code, XCOM program and experimental data: a comparison study, Nucl. Instrum. Methods Phys. Res. A 735 (2014) 207–217, https://doi.org/10.1016/j.nima.2013.09.027s.

[49] H.T. Tekin, A. Ghada, Y.S. Rammah, M.A. Emad, T.A. Fatema, S.B. Duygu, E. Wiam, M.H. Hesham, Z. Shams, A.M. Issa, G. Kilic, E. Antoaneta, Transmission factors, mechanical, and gamma ray attenuation properties of barium-phosphate-tungsten glasses: incorporation impact of WO3, Optik 267 (2022) 169643, https://doi.org/10.1016/j.ijleo.2022.169643.
[50] M.J. Berger, J.H. Hubbell, XCOM: Photon Cross Sections Database, Web Version 1.2, 1999, Originally published as NBSIR 87-3597 XCOM: Photon Cross Sections on a Personal Computer, Washington, DC, 1987. Available from: http://physics.nist.gov/xcom.
[51] Shamsan S. Obaid, Dhammajyot K. Gaikwad, Pravina P. Pawar, Determination of gamma ray shielding parameters of rocks and concrete, Radiat.Physi.Chem. (2017) 1–5, https://doi.org/10.1016/j.radphyschem.2017.09.022.
[52] M.M. Rafieia, H. Tavakoli-Anbaran, M. Kurudirek, A detailed investigation of gamma-ray energy absorption and dose buildup factor for soft tissue and tissue equivalents using Monte Carlo simulation, Radiat. Phys. Chem. 177 (2020) 109118, https://doi.org/10.1016/j.radphyschem.2020.109118, 1-7.